Eur. Phys. J. B **54**, 449–456 (2006)
DOI: 10.1140/epjb/e2007-00023-9

THE EUROPEAN PHYSICAL JOURNAL B

Analytical determination of the Landau-Ginzburg parameters of (100) metal homoepitaxial systems

G. Petsos[a] and H.M. Polatoglou

Department of Physics, Aristotle University of Thessaloniki, 54124 Thessaloniki, Greece

Received 13 April 2006 / Received in final form 20 December 2006
Published online 3 February 2007 –

Abstract. In the initial stages of homoepitaxial growth on the (100) surface of metals such as Ag, Fe, Cu, Ni, and Pd, where the clean surface does not reconstruct, two-dimensional islands with compact, near-square shapes are formed. In order to determine the phenomenological material parameters of the nonlinear and nonlocal Landau-Ginzburg theory, which describes the metal homoepitaxial systems mentioned above, an atomistic model for these systems is developed. Based on this model, we derive analytical relationships between the Landau-Ginzburg parameters A, B, C, and D, and the parameters of the homoepitaxial system (such as coverage, first-neighbour interaction energy, etc.). We find that the Landau-Ginzburg parameters of the system depend on the specific material as well as on the coverage of the surface. We then apply the method to the Ag/Ag(100) system.

PACS. 68.47.De Metallic surfaces – 61.50.Ah Theory of crystal structure, crystal symmetry; calculations and modeling – 64.60.Qb Nucleation

1 Introduction

Surface phenomena are important in science and industry, and their study and exploitation have lead to a revolution in many fields [1]. Their study has been greatly advanced with the development of the scanning-tunnelling microscope and its extensions such as the atomic-force microscope and the scanning-probe microscope in general. The atomic resolution offered by these tools has enormously increased our knowledge of the structure and dynamics of surfaces [2]. In combination with high vacuum conditions, and controlled coverage and sample temperature, it is possible to study not only adatom dynamics and thermodynamic behaviour but also the initial states of nucleation and growth. As the possible combinations of surface, adatom type, and surface density are enormous, so are the possible outcomes. Important effects following the interaction between adatoms and surfaces include the mediation of these interactions due to surface strain and electronic effects. There is a need to study these cases over many different length scales and in various degrees of detail. Since the atomic interactions are different at the surface than in the bulk, and new types of interactions are possible, there is also a need to extend the modelling of these interactions. In addition, the modelling of adatom dynamics requires taking into account a large number of atoms and is therefore very demanding in terms of computer resources. All of this has resulted in a wealth of methods, new and old, being applied, ranging from continuum theories to atomistic models, from semiempirical to ab initio, and from classical methods to quantum-mechanical treatments.

A system that has attracted a lot of attention is that of homoepitaxy on metallic and semiconducting surfaces. Concerning the effect on the adatom dynamics, it was found that for a given number of adatoms at high temperatures, the adatoms are quite mobile and do not form islands, whilst at lower temperatures they do form islands [3]. The special case of the initial stages of homoepitaxial nucleation and growth on the (100) surfaces of metals such as Ag, Fe, Cu, Ni, and Pd, where the surface does not reconstruct and two-dimensional islands with compact, near-square shapes are formed, has been studied [4–11]. Most of the modelling for such cases is at the atomic level. On the other hand, for the case of spiral growth on surfaces [12], the nonlinear, nonlocal, time-dependent Landau-Ginzburg theory was used. In another work, the nonlinear, nonlocal, time-dependent Landau-Ginzburg theory was combined with a stochastic process in order to study the growth of square islands on the (100) surface of Ag [13].

In this paper, we develop a simple atomistic model for the metallic homoepitaxial systems mentioned above, and based on this model we derive analytical relationships between the parameters of the system (such as coverage, first-neighbour interaction energy, etc.) and the

[a] e-mail: gpetsos@physics.auth.gr

phenomenological, positive and temperature-independent Landau-Ginzburg parameters of the system. We believe that this is the first example of the provision of analytical relationships between the parameters of the homoepitaxial system and the Landau-Ginzburg parameters of the system. We should also emphasise that we are interested in small coverages of the surface, which means that the total number of adatoms is much smaller than the number of available lattice adsorption sites on the surface.

In order to determine the relationships between the Landau-Ginzburg parameters of the system and the homoepitaxial parameters, we consider two different limiting equilibrium states of the system. In the first state, all of the adatoms are free on the surface and there are no bonds between them. This state corresponds to phase 1. In the second state, all of the adatoms have formed a two-dimensional island with a compact, near-square shape, which contains a small number of perimetric vacancies. This state of the system corresponds to phase 2. Then we calculate both atomistically and using the Landau-Ginzburg theory, the free energy changes between these two phases. The condition of coincidence between these two approaches results in a system of four equations with four unknowns: the Landau-Ginzburg parameters A, B, C, and D of the system. By solving this system of equations with respect to the Landau-Ginzburg parameters, we finally find four analytical relations between the Landau-Ginzburg parameters A, B, C, and D, and the parameters of the homoepitaxial system. Our main conclusion is that the Landau-Ginzburg parameters of the homoepitaxial system depend on the specific material as well as on the coverage of the surface. We perform an application of the whole procedure to the case of an Ag/Ag(100) system.

Our paper is organised as follows. In Section 2, we describe the atomistic model and we calculate the total free energy change of the system when a two-dimensional island is formed on the surface. In Section 3, we determine the density of the two-dimensional island. Then, in Section 4 we develop the Landau-Ginzburg theory to describe the (100) metallic homoepitaxial systems and we also derive the analytical relationships between the Landau-Ginzburg parameters and the parameters of the homoepitaxial system. Finally, in Section 5 we summarise our findings.

2 The atomistic model

We consider n adatoms on a (100) metal surface that contains N four-fold hollow adsorption sites, and we study two different limiting equilibrium states of the system. As we can see in Figures 1a and 1b, in the first state all of the adatoms are free on the surface and there are no bonds between them (phase 1), whereas in the second state all of the adatoms have formed a square island that contains a small number of perimetric vacancies (phase 2).

The internal energy U_1 of phase 1 is given by

$$U_1 = n\varepsilon_2, \tag{1}$$

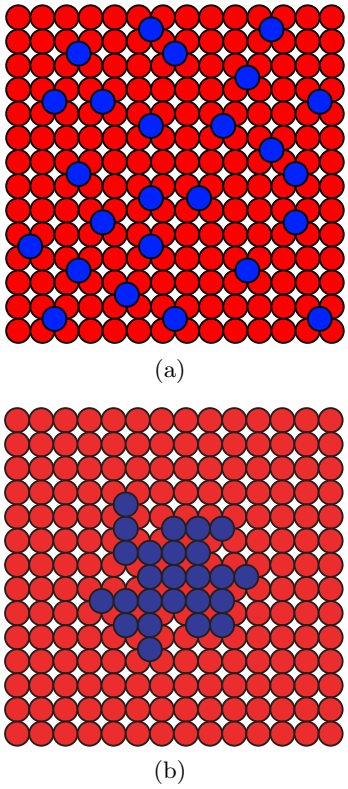

(a)

(b)

Fig. 1. (a) Schematic illustration of the state where all adatoms are free on the surface. This state of the system corresponds to phase 1. (b) Schematic illustration of the state where all adatoms have formed a compact island with a near-square shape. This state of the system corresponds to phase 2.

where ε_2 is the interaction energy between an adatom and the surface. The entropy S_1 of this state is given by

$$S_1 = k_B \ln\left[\frac{(N-5n+5)!}{n!\,(N-6n+5)!}\right], \tag{2}$$

where $k_B = 8.62 \times 10^{-5}$ eV/K is Boltzmann's constant and the fraction $\frac{(N-5n+5)!}{n!(N-6n+5)!}$ is the statistical weight Ω of this state, which is equal to the number of ways in which the n free adatoms can occupy the $N-5(n-1)$ lattice sites available on the surface. The Helmholtz free energy F_1 of this equilibrium state at a temperature T is given by

$$F_1 = U_1 - TS_1 = n\varepsilon_2 - Tk_B \ln\left[\frac{(N-5n+5)!}{n!\,(N-6n+5)!}\right], \tag{3}$$

and the coverage $\theta = n/N$ must satisfy the condition: $\theta < 1/6 + 1/N$.

In phase 2, we consider that the concentration of the perimetric vacancies is small. Hence, to a first approximation we can consider that for every vacancy, two first-neighbour bonds are broken (three first-neighbour bonds are broken when a perimetric atom leaves the island and one first-neighbour bond is created between this atom and the island). In addition, we should emphasise that the perimetric atoms that leave the island remain attached to

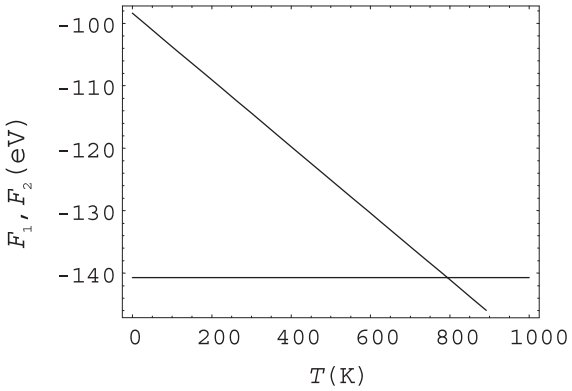

Fig. 2. The dependence of the free energies F_1 and F_2 on temperature. F_1 is the free energy of phase 1 and decreases linearly as the temperature increases, whereas F_2 is the free energy of phase 2 and to a first approximation is temperature-independent.

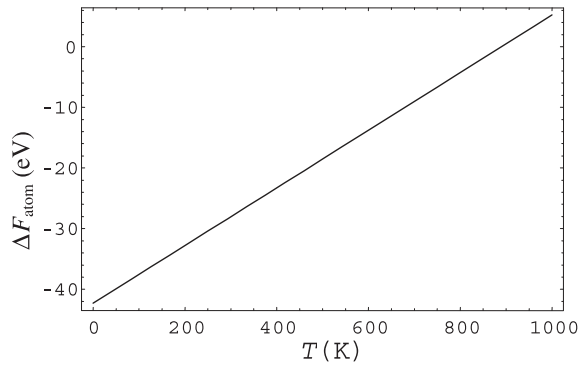

Fig. 3. The dependence of the free energy change $\Delta F_{atom} = F_2 - F_1$ on temperature. The free energy change increases linearly as the temperature increases and it vanishes at the transition temperature T_1.

the island and there are no free adatoms in phase 2. Hence, the internal energy U_2 of a square island that contains $n = n_1^2$ atoms and N_v perimetric vacancies is given by

$$U_2 = 2n\varepsilon_1 - 2\sqrt{n}\varepsilon_1 - 8\lambda\sqrt{n}\varepsilon_1 + n\varepsilon_2, \tag{4}$$

where ε_1 is the first-neighbour interaction energy between the adatoms, and $\lambda = N_v/(4\sqrt{n})$ is the concentration of vacancies. By setting $\lambda = 0$ in equation (4) we can find the internal energy of a square island with no vacancies. Bearing in mind that the vacancy concentration is small, we can consider the entropic term to be very small for this state. Hence, the Helmholtz free energy F_2 of this state is given by

$$F_2 \cong U_2 = 2n\varepsilon_1 - 2\sqrt{n}\varepsilon_1 - 8\lambda\sqrt{n}\varepsilon_1 + n\varepsilon_2. \tag{5}$$

The total free energy change $\Delta F_{atom} = F_2 - F_1$ is given by

$$\Delta F_{atom} = 2\varepsilon_1\left(n - \sqrt{n}\right) - 8\lambda\sqrt{n}\varepsilon_1 + Tk_B \ln\left[\frac{(N-5n+5)!}{n!\,(N-6n+5)!}\right], \tag{6}$$

where we have used the subscript "atom" because we calculate this energy atomistically. In Figure 2, the dependence of F_1 and F_2 on temperature is shown, whereas the temperature dependence of ΔF_{atom} for the Ag/Ag(100) system is shown in Figure 3. The lattice constant of Ag is $a = 4.09$ Å, while the cohesive energy per atom in the bulk is equal to 2.95 eV [14,15]. Hence, the first-neighbour interaction energy is $\varepsilon_1 = -2.95/12$ eV $= -0.246$ eV since every atom in the bulk fcc lattice has 12 first neighbours. The interaction energy ε_2 between an adatom and the surface (which contains four-fold hollow adsorption sites) is taken to be $\varepsilon_2 = 4\varepsilon_1 = -0.984$ eV. Also, we choose $N = 10^4$ adsorption sites, $n = 100$ adatoms and $\lambda = 0.1$. These are then the values of the parameters a, ε_1, ε_2, N, n, and λ of the homoepitaxial system that will be considered in this paper.

The transition temperature T_1 at which $\Delta F_{atom} = 0$ is given by

$$T_1 = \frac{8\lambda\sqrt{n}\varepsilon_1 - 2\varepsilon_1\left(n - \sqrt{n}\right)}{k_B \ln\left[\frac{(N-5n+5)!}{n!(N-6n+5)!}\right]}. \tag{7}$$

For $T < T_1$, phase 2 is more stable, whereas phase 1 is more stable for $T > T_1$. We should mention that our model is equivalent to the classical two-dimensional Ising lattice-gas model with first-neighbour attractive interactions. As expected, the transition temperature T_1 (which is the temperature where the system enters the two-phase coexistence regime) depends on the material as well as on the coverage $\theta = n/N$ of the surface. In order to illustrate the validity of our analysis, we compare the transition temperature T_1 against the Ising lattice-gas model prediction (Onsager's solution) for the Ag/Ag(100) system. In Figure 4, the coverage-temperature phase diagrams for the two-dimensional Ising lattice-gas model and our atomistic model are shown. As is well-known, the line that separates the two regimes (binodal) for the two-dimensional Ising lattice-gas model (Onsager's solution) can be calculated exactly and is given by [16]

$$T = \frac{2J}{k_B} \frac{1}{\ln\left[\sqrt{\frac{1}{1-(2\theta-1)^8}} + \sqrt{\frac{1}{1-(2\theta-1)^8} + 1}\right]}, \tag{8}$$

where k_B is Boltzmann's constant, θ is the coverage, and $J = -\varepsilon_1/4$. As can be seen in Figure 4, the agreement is quite good for small coverages although disagreement occurs at higher coverages. This is not unexpected, since our atomistic model is quite simple in the sense that there are no first-neighbour interactions between the adatoms in phase 1 (all of the adatoms are isolated). This is a good approximation for small coverages, but at higher coverages we expect the presence of significant first-neighbour interactions between the adatoms. Thus, in our atomistic model, the transition temperature T_1 can be very high

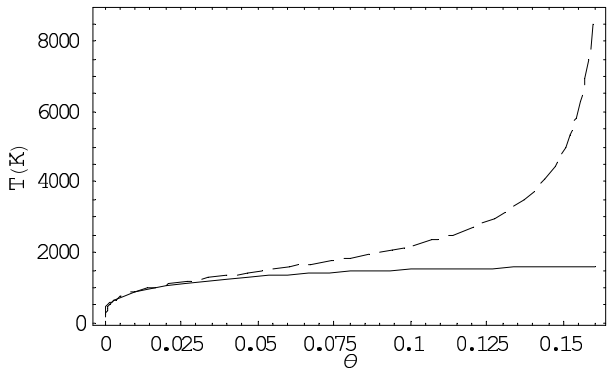

Fig. 4. The coverage-temperature phase diagrams for the two-dimensional Ising lattice-gas model (Onsager's solution) and the atomistic model. The solid line represents Onsager's solution and the dashed line represents the atomistic model.

when the coverage is relatively high, and the restriction of isolated adatoms in phase 1 is fulfilled. To summarise, we conclude that in the small-coverage regime (which is the regime that we are interested in) our predictions agree quite well to that of Onsager's solution.

It would be very interesting if we were able to compare the transition temperature T_1 with experimental observations. As far as we know, there has been no experimental determination of the transition temperature for (100) metal homoepitaxial systems. Nevertheless, we are aware of a situation similar to that presented here: Tromp and Mankos [3] have successfully measured the concentration of Si atoms, on very large step-free regions of a Si(001) surface, as a function of temperature. At high temperatures in the range of 750–1050 °C, the surface contained only the adatom lattice gas, which was too dilute and too mobile to be observed directly. The sample was then rapidly quenched, and as the temperature dropped, the adatom gas became supersaturated, and the nucleation and growth of two-dimensional islands was observed in real time. Hence, at low temperatures the surface contained only a distribution of two-dimensional islands. By measuring the fractional area of the terrace covered by the two-dimensional islands, they were able to determine the adatom concentration at the initial high temperature. Of course, they did not measure the transition temperature between the two states (adatom gas and islands) as a function of coverage, but the similarity between their system and the atomistic model presented here is clear. At high temperatures there is only the adatom lattice gas, whereas at low temperatures only two-dimensional islands are formed. Finally, we conclude that an experimental determination of the transition temperature (for (100) metal homoepitaxial systems) as a function of coverage is something that remains to be done.

3 The density of the two-dimensional island

In this section we describe the method with which it is possible to determine the density of a compact, two-dimensional, near-square island, which contains $n = n_1^2$ atoms and N_v perimetric vacancies.

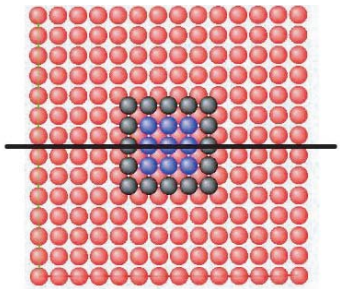

Fig. 5. Schematic illustration of a lattice line of the island in the horizontal direction x. At the middle of each segment of length a there is an atom of the island. The perimetric atoms are shown as grey in colour.

As can be seen in Figure 5, in order to calculate the density in the horizontal direction x, we consider a lattice line of the island (with lattice constant a) that contains n_1 atoms, and then divide this line into n_1 segments of length a in such a way that there is an atom at the middle of any segment. Placing the origin of the axes on the first atom from the left, we find that the discrete density $\rho_{dis}(x)$ for the points from $x = a$ to $x = (n_1 - 2)a$ (where there are no vacancies) is equal to $\rho_{max} = 1$ atom/a. For the points $x = 0$ and $x = (n_1 - 1)a$ (these atoms being coloured grey), where the detachment of an atom and the subsequent creation of a vacancy is possible, the density $\rho_{dis}(x)$ is equal to

$$\rho_{dis}(0) = \rho_{dis}((n_1 - 1)a) = (1 - \lambda)\rho_{max}. \quad (9)$$

The density at these points is different because at the island's edges there is a probability $(1 - \lambda)$ that an atom will remain at the edge of the island. In the same way, the density $\rho_{dis}(x)$ at the points $x = -a$ and $x = n_1 a$ is given by

$$\rho_{dis}(-a) = \rho_{dis}(n_1 a) = \lambda\rho_{max}. \quad (10)$$

In summary, we find that the discrete density $\rho_{dis}(x)$ is given by:

$$\begin{aligned} \rho_{dis}(x) &= 0, \forall x < -a, \\ \rho_{dis}(x) &= 0, \forall x > n_1 a, \\ \rho_{dis}(x) &= \rho_{max}, \forall x = a, ..., (n_1 - 2)a, \\ \rho_{dis}(0) &= \rho_{dis}((n_1 - 1)a) = (1 - \lambda)\rho_{max}, \\ \rho_{dis}(-a) &= \rho_{dis}(n_1 a) = \lambda\rho_{max}. \end{aligned} \quad (11)$$

As expected, the density change at the island's edges is determined by the concentration λ of the vacancies. For $\lambda = 0$, we find $\rho_{dis}(0) = \rho_{dis}((n_1 - 1)a) = \rho_{max}$ and $\rho_{dis}(-a) = \rho_{dis}(n_1 a) = 0$, which means that the island is perfectly square. In Figure 6, a graph of the discrete density $\rho_{dis}(x)$ is shown.

It is possible, for small λ, to approximate very well the discrete density $\rho_{dis}(x)$ by the continuous density $\rho_{cont}(x)$, which is given by

$$\rho_{cont}(x) = \rho_{max}\mathrm{Exp}\left[\frac{-(x-\mu)^{2\kappa}}{d^{2\kappa}}\right], \quad (12)$$

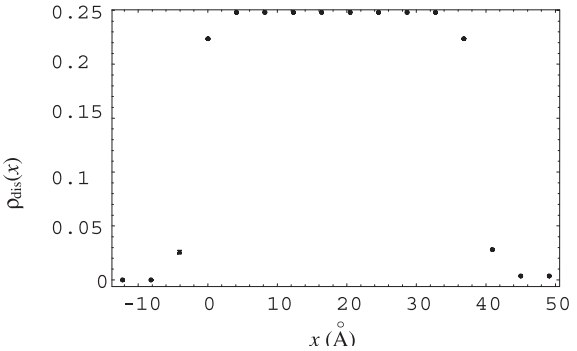

Fig. 6. A graph of the discrete density $\rho_{dis}(x)$. The density change at the island's edges is determined by the concentration λ of the vacancies.

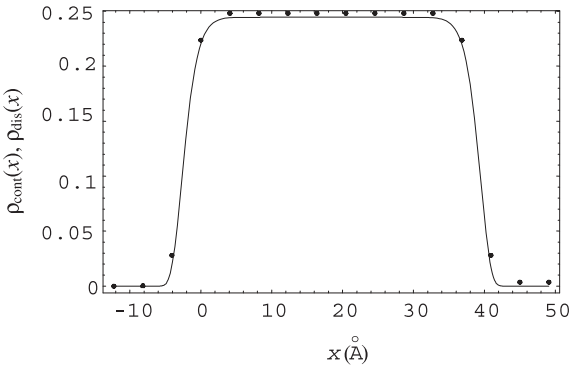

Fig. 7. Comparison between the discrete and the continuous densities. The symbols show the discrete density while the solid line indicates the continuous density. It can be seen that the agreement between them is very good.

when:

$$\mu = \frac{n_1 - 1}{2} a, \tag{13}$$

$$\kappa = \frac{1}{2} \frac{\ln\left[\frac{\ln(1-\lambda)}{\ln\lambda}\right]}{\ln\left(\frac{n_1-1}{n_1+1}\right)}, \tag{14}$$

and

$$d = \left[\frac{(-\mu)^{2\kappa}}{\ln\left(\frac{1}{1-\lambda}\right)}\right]^{\frac{1}{2\kappa}}. \tag{15}$$

The parameter κ in equation (14) is rounded in order to take integer values. The condition that the continuous density $\rho_{cont}(x)$ is a maximum and equal to ρ_{max} at the middle μ of the island determines equation (13), whereas equations (14) and (15) are determined by the condition that the continuous density $\rho_{cont}(x)$ is equal to the discrete density at the points $x = -a$ and $x = 0$ or equivalently at $x = (n_1 - 1)a$ and $x = n_1 a$. Using equations (13–15) we find $\mu = 18.405$ Å, $\kappa = 8$, and $d = 21.184$ Å. As we can see in Figure 7, the continuous density $\rho_{cont}(x)$ approximates very well the discrete density $\rho_{dis}(x)$ for small λ.

Due to symmetry, the continuous density $\rho_{cont}(y)$ in the vertical direction y is given by

$$\rho_{cont}(y) = \rho_{max} \mathrm{Exp}\left[\frac{-(y-\mu)^{2\kappa}}{d^{2\kappa}}\right], \tag{16}$$

where the parameters μ, κ, and d are given by equations (13–15) respectively, and $\rho_{max} = 1$ atom/a. Finally, the continuous density $\rho_{cont}(x, y)$ of the near-square two-dimensional island is given by

$$\rho_{cont}(x, y) = \rho_{cont}(x)\rho_{cont}(y) = \rho^2_{max} g(x, y), \tag{17}$$

where $\rho^2_{max} = 1$ atom/a^2 and

$$g(x, y) = \mathrm{Exp}\left[-\frac{(x-\mu)^{2\kappa} + (y-\mu)^{2\kappa}}{d^{2\kappa}}\right].$$

In Figure 8a, a graph of $\rho_{cont}(x, y)$ is shown.

By integrating $\rho_{cont}(x, y)$ over the entire surface, we find

$$\int_{-\frac{\sqrt{N}}{2}\alpha}^{\frac{\sqrt{N}}{2}a} \int_{-\frac{\sqrt{N}}{2}\alpha}^{\frac{\sqrt{N}}{2}\alpha} \rho_{cont}(x, y) dx dy = 100.467 \text{ atoms},$$

which is in very good agreement with the value of $n = 100$ atoms.

4 Determination of the Landau-Ginzburg parameters

Within the framework of the nonlinear and nonlocal Landau-Ginzburg theory, the total free energy change of the system when a near-square island is formed on a surface is a functional of the order parameter. Based on previous Landau-Ginzburg studies on binary fluids, binary alloys [17], and structural phase transitions [18–21], we adopt the following free energy functional:

$$\Delta F_{LG} = \iint \left[\frac{1}{2} A\delta T\sigma^2 - \frac{1}{3} B\sigma^3 + \frac{1}{4} C\sigma^4 + \frac{1}{2} D\left(\frac{\partial\sigma}{\partial x}\right)^2 + \frac{1}{2} D\left(\frac{\partial\sigma}{\partial y}\right)^2\right] dxdy, \tag{18}$$

where A, B, C, and D are positive, temperature-independent phenomenological parameters of the system, $\delta T = T - \tilde{T}_c$, the critical temperature at which phase 1 becomes unstable is $\tilde{T}_c$, and $\sigma(x, y) = \frac{\rho_{cont}(x,y) - \rho_0}{\rho_0}$ is the order parameter of the system. $\rho_0 = n/(Na^2)$ is the density of phase 1 and the integration is performed over the entire surface. The local free energy density $f_L = \frac{1}{2} A\delta T\sigma^2 - \frac{1}{3} B\sigma^3 + \frac{1}{4} C\sigma^4$ has one minimum at $\sigma = 0$ corresponding to phase 1, and another minimum at a value where $\sigma > 0$. For $\delta T = 0$ ($T = \tilde{T}_c$), the free energy density barrier vanishes and phase 1 becomes unstable. The

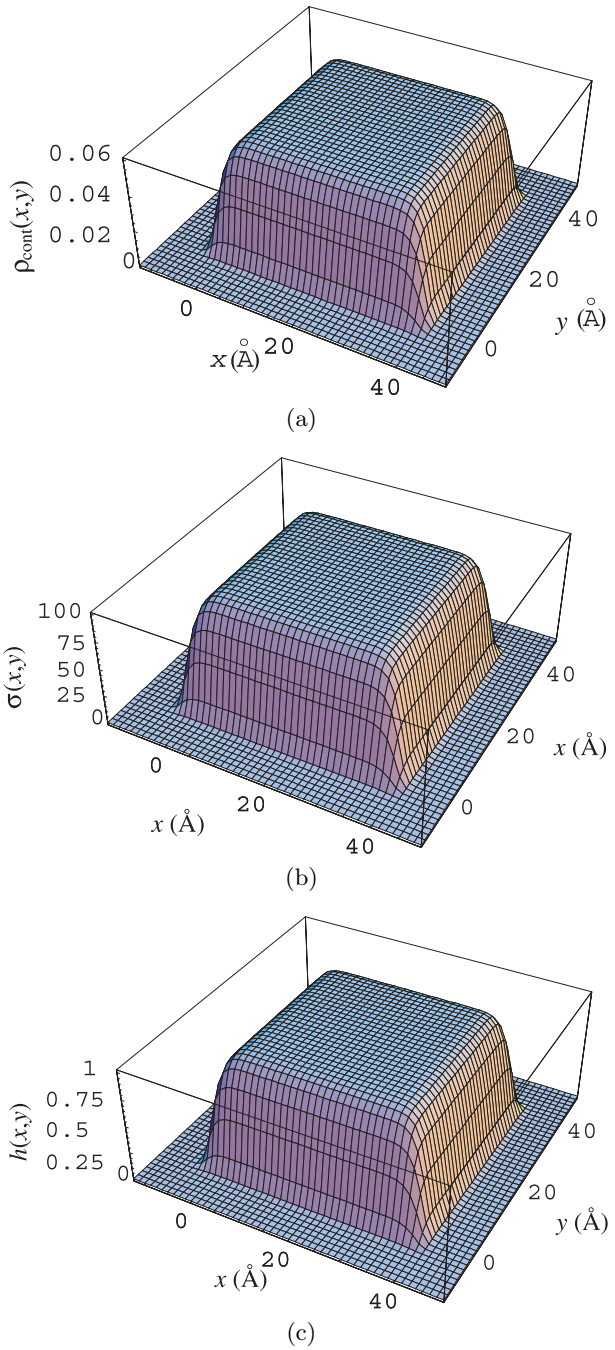

Fig. 8. (a) A graph of the continuous density $\rho_{cont}(x, y)$ of a two-dimensional island with a compact, near-square shape. (b) A graph of the order parameter $\sigma(x, y)$ of the homoepitaxial system. (c) A graph of the function $h(x, y)$ for the homoepitaxial system.

gradient terms in the free energy functional represent the vacancy contribution to the total free energy change of the system. Also, as mentioned in the introduction, we are interested in small coverages of the surface. Hence, we do not take into account the dynamics of the growth of phase 2. What we essentially do is compute the free energy differences between the two phases and study their relative stability. In order to do this, we use the nonlinear and nonlocal Landau-Ginzburg theory instead of the classical nucleation theory. The free energy functional given by equation (18) describes the square symmetry in the perpendicular directions x and y.

In Figure 8b, a graph of $\sigma(x, y)$ is shown. It is easily demonstrated that the order parameter can be written as

$$\sigma(x, y) = \sigma_{max} h(x, y), \tag{19}$$

where

$$\sigma_{max} = \frac{\rho_{max}^2 - \rho_0}{\rho_0} = \frac{1 - \theta}{\theta} \tag{20}$$

is the maximum value of the order parameter, and the function $h(x, y)$ is given by

$$h(x, y) = \frac{\rho_{cont}(x, y) - \rho_0}{\rho_{max}^2 - \rho_0}. \tag{21}$$

In Figure 8c, a graph of the function $h(x, y)$ is shown. The order parameter takes values between –1 and σ_{max}, whereas the function $h(x, y)$ varies between –1/ σ_{max} and 1. Both of these are dimensionless.

Inserting equation (19) into equation (18), we find that

$$\Delta F_{LG} = \frac{1}{2}\tilde{A}\sigma_{max}^2 - \frac{1}{3}\tilde{B}\sigma_{max}^3 + \frac{1}{4}\tilde{C}\sigma_{max}^4, \tag{22}$$

where:

$$\tilde{A} = I_1 A\delta T + DI_4, \tag{23}$$

$$\tilde{B} = I_2 B, \tag{24}$$

$$\tilde{C} = I_3 C, \tag{25}$$

$$I_1 = \iint h^2(x, y)dxdy, \tag{26}$$

$$I_2 = \iint h^3(x, y)dxdy, \tag{27}$$

$$I_3 = \iint h^4(x, y)dxdy, \tag{28}$$

and

$$I_4 = \iint \left[\left(\frac{\partial h}{\partial x}\right)^2 + \left(\frac{\partial h}{\partial y}\right)^2\right] dxdy. \tag{29}$$

The total free energy change ΔF_{LG} has a minimum at $\sigma_{max} = 0$, which corresponds to phase 1, and another minimum at a value where $\sigma_{max} > 0$, which corresponds to phase 2. The relative stability of the two phases depends on the values of the parameters $\tilde{A}$, $\tilde{B}$, and $\tilde{C}$. In Figure 9a, a graph of the total free energy change ΔF_{LG} for the values $\tilde{A} = 0.2$, $\tilde{B} = 1$, and $\tilde{C} = 1$ is shown. The local minimum of Δ_{LG} at $\sigma_{max} = 0$ corresponds to phase 1, whereas the global minimum at a value $\sigma_{max} > 0$ corresponds to phase 2.

Until now, we have calculated the total free energy change of the system atomistically and from the Landau-Ginzburg theory. In order to have agreement between these two approaches, the free energy changes must be equal at any temperature. This is true when $\Delta F_{LG} = 0$ at $T = T_1$ (T_1 being the transition temperature given by

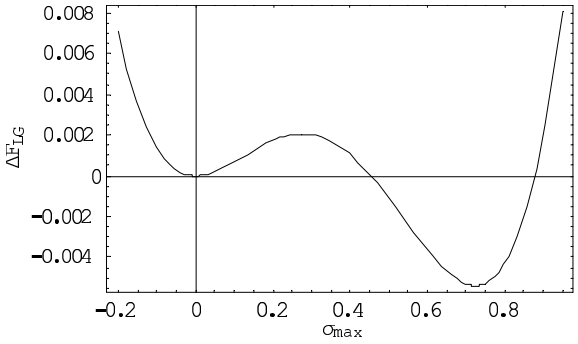

(a)

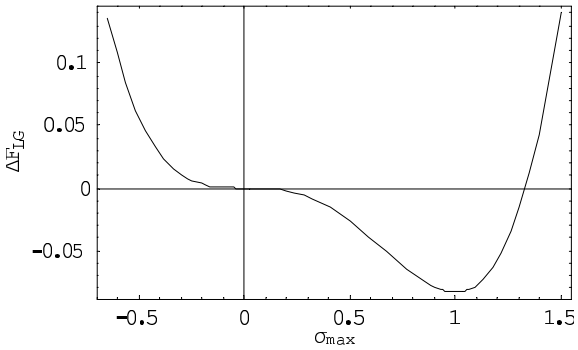

(b)

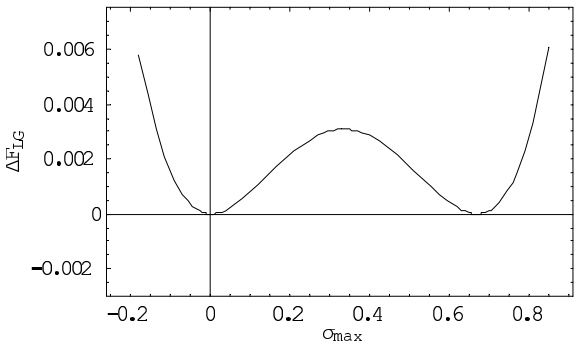

(c)

Fig. 9. (a) A graph of the total free energy change ΔF_{LG} of the system for the values $\tilde{A} = 0.2$, $\tilde{B} = 1$, and $\tilde{C} = 1$. The local minimum at $\sigma_{max} = 0$ corresponds to phase 1, whereas the global minimum at $\sigma_{max} > 0$ corresponds to phase 2. (b) A graph of the total free energy change ΔF_{LG} of the system for the values $\tilde{A} = 0$, $\tilde{B} = 1$, and $\tilde{C} = 1$. As can be seen, the free energy barrier vanishes. The point $\sigma_{max} = 0$ is a turning point of ΔF_{LG}. (c) A graph of the total free energy change ΔF_{LG} of the system for the values $\tilde{A} = 2/9$, $\tilde{B} = 1$, and $\tilde{C} = 1$. It can be seen that the two minima of ΔF_{LG} have the same value of free energy.

Eq. (7)) and the derivatives of equations (6) and (22) with respect to T are equal. This is true when

$$\frac{1}{2}\left[I_1 A\left(T_1 - \tilde{T}_c\right) + DI_4\right] - \frac{1}{3}I_2 B\sigma_{max} + \frac{1}{4}I_3 C\sigma_{max}^2 = 0, \tag{30}$$

and

$$A = \frac{2S_1}{I_1\sigma_{max}^2}. \tag{31}$$

Hence, we have determined the phenomenological Landau-Ginzburg parameter A so far. The critical temperature T_c for the formation of an island with perimetric vacancies (phase 2) is determined by the condition that $\tilde{A} = 0$. When this is fulfilled, the total free energy barrier vanishes, and the point $\sigma_{max} = 0$ is a turning point of ΔF_{LG}. In Figure 9b, a graph of ΔF_{LG} for the values $\tilde{A} = 0$, $\tilde{B} = 1$, and $\tilde{C} = 1$ is shown. As can be seen, the free energy barrier vanishes. From the condition $\tilde{A} = 0$ we find that

$$\tilde{T}_c - T_c = \frac{DI_4}{AI_1}. \tag{32}$$

From the above relation we see that $\tilde{T}_c > T_c$ always. The transition temperature T_1 is determined by the condition

$$\tilde{A} = \frac{2}{9}\frac{\tilde{B}^2}{\tilde{C}}. \tag{33}$$

When this condition is fulfilled, the value of the total free energy change ΔF_{LG} at the minimum where $\sigma_{max} > 0$ is equal to zero, and the two minima of ΔF_{LG} have the same value of free energy. In Figure 9c, a graph of ΔF_{LG} for the values $\tilde{A} = 2/9$, $\tilde{B} = 1$, and $\tilde{C} = 1$ is shown. As can be seen, the two minima of ΔF_{LG} have the same amount of free energy.

Combining equations (32) and (33), we find that

$$T_1 - T_c = \frac{2}{9}\frac{I_2^2 B^2}{I_1 I_3 AC}. \tag{34}$$

Using equations (30–32) and (34), we can find the other three positive phenomenological parameters B, C, and D of the homoepitaxial system. We find that:

$$B = \frac{6S_1\left(T_1 - T_c\right)}{I_2\sigma_{max}^3}, \tag{35}$$

$$C = \frac{4S_1\left(T_1 - T_c\right)}{I_3\sigma_{max}^4}, \tag{36}$$

$$D = \frac{2S_1\left(\tilde{T}_c - T_c\right)}{I_4\sigma_{max}^2}. \tag{37}$$

From equation (7), we can find the transition temperature T_1. Within the framework of our atomistic model, it is not possible to determine the critical temperatures T_c and $\tilde{T}_c$. It is clear that the Landau-Ginzburg parameters A, B, C, and D of the system depend on the specific material as well as on the coverage θ of the surface.

5 Conclusions

We have considered the initial stages of homoepitaxial growth on the (100) surface of such metals as Ag, Fe, Cu, Ni, and Pd, where two-dimensional islands with compact, near-square shapes are formed. We have considered

two limiting equilibrium states of the system. In the first state, all of the adatoms are free on the surface and there are no bonds between them, whereas in the second state all of the adatoms have formed a two-dimensional island with compact, near-square shape. As expected, the transition temperature for the formation of the island depends on the material as well as on the surface coverage. We have developed a method for a determination of the density of a two-dimensional island with a compact, near-square shape.

We have also derived analytical relationships between the parameters of the homoepitaxial system (such as coverage, first-neighbour interaction energy, etc.) and the phenomenological, positive and temperature-independent Landau-Ginzburg parameters A, B, C, and D of the system. We have shown that the Landau-Ginzburg parameters depend on the specific material as well as on the coverage of the surface. In order to illustrate the capability of the procedure, we have applied it to the Ag/Ag(100) system.

References

1. Harald Ibach, *Physics of Surfaces and Interfaces* (Springer, Berlin, 2006)
2. *Surface Analysis – The Principal Techniques*, edited by J.C. Vickerman (John Wiley & Sons, 1997)
3. R.M. Tromp, M. Mankos, Phys. Rev. Lett. **81**, 1050 (1998)
4. C.R. Stoldt et al., Prog. Surf. Sci. **59**, 67 (1998)
5. C.-M. Zhang et al., Surf. Sci. **406**, 178 (1998)
6. M.C. Bartelt, J.W. Evans, Surf. Sci. **423**, 189 (1999)
7. S. Frank et al., Phys. Rev. B **66**, 155435 (2002)
8. Da-Jiang Liu, J.W. Evans, Phys. Rev. B **66**, 165407 (2002)
9. Maozhi Li, J.W. Evans, Surf. Sci. **546**, 127 (2003)
10. Maozhi Li, M.C. Bartelt, J.W. Evans, Phys. Rev. B **68**, 121401(R) (2003)
11. Maozhi Li, J.W. Evans, Phys. Rev. B **69**, 035410 (2004)
12. I.S. Aranson et al., Phys. Rev. Lett. **80**, 1770 (1998)
13. G. Petsos, V. Vargiamidis, Comput. Mater. Sci. **17**, 505 (2000)
14. N.W. Aschroft, N.D. Mermin, *Solid State Physics* (College Edition, Saunders College Publishing, 1976)
15. C. Kittel, *Introduction to Solid State Physics*, 5th edition (John Wiley & Sons, Inc., 1976)
16. M.E.J. Newman, G.T. Barkema, *Monte Carlo Methods and Statistical Physics* (Oxford University Press, New York, 1999)
17. J.D. Gunton, M. San Miguel, P.S. Sahni, in *Phase Transitions and Critical Phenomena*, edited by C. Domb, J.L. Lebowitz (Academic Press Inc., London, 1983), p. 269
18. A.C.E. Reid, R.J. Gooding, Phys. Rev. B **50**, 3588 (1994)
19. B.P. van Zyl, R.J. Gooding, Phys. Rev. B **54**, 15700 (1996)
20. B.P. van Zyl, R.J. Gooding, Metall. Mater. Trans. A **27**, 1203 (1996)
21. Y.A. Chu et al., Metall. Mater. Trans. A **31**, 1321 (2000)